4. Yeo, R. S.; Orehotsky, J.; Visscher, W.; Srinivasan, S. *J. Electrochem. Soc.* **1981**, *128*, 1900.
5. Park, S.; Mho, S.; Chi, E.; Kwon, Y.; Yeo, I. *Bull. Korean Chem. Soc.* **1995**, *16*, 82.
6. Ardizzone, S.; Falciola, M.; Trasatti, S. *J. Electrochem. Soc.* **1985**, *136*, 1545.
7. Melsheimer J.; Ziegler, K. *Thin Solid Films* **1988**, *163*, 301.
8. Kobayashi, H.; Nagata, M.; Kanno, R.; Kawamoto, Y. *Mater. Res. Bull.* **1994**, *29*, 1271.
9. Dabrowski, B.; Jorgensen, J.; Minks, D.; Pei, S.; Richards, K.; Vanfleet, H.; Kecker, K. *Physica C* **1989**, *162*, 99.
10. Egdell, R. G.; Goodenough, J. B.; Hamnett, A.; Naish, C. C. *J. Chem. Soc., Faraday Trans.* **1983**, *1*, 79.
11. Gokagac G.; Kennedy, B. J. *J. Electroanal. Chem.* **1993**, *353*, 71.
12. Bard, A. J.; Faulkner, L. R. *Electrochemical Methods*; Wiley: New York, 1980; p 106.
13. Bockris, J. O'M.; Otagawa, T. *J. Electrochem. Soc.* **1984**, *131*, 290.
14. Matsumoto, Y.; Manabe, H.; Sato, E. *J. Electrochem. Soc.* **1980**, *127*, 811.
15. Rasiyah, P.; Tseung, A. C. C. *J. Electrochem. Soc.* **1983**, *130*, 2384.
16. Beyerlein, R. A.; Horowitz, H. S.; Longo, J. M.; Leonowicz, E.; Jorgensen, J. D.; Rotella, F. J. *J. Solid State Chem.* **1984**, *51*, 253.
17. England, W. A.; Cross, M. G.; Mamnett, M.; Wiseman, P. J.; Goodenough, J. B. *Solid State Ionics* **1980**, *1*, 231.
18. Fujishima, A.; Honda, K. *Nature (London)* **1972**, *238*, 37.
19. Gennero de Chialvo, M. R.; Chialvo, A. C. *Electrochim. Acta* **1988**, *33*, 825.

Ligand Field Approach to $4d^1$ Magnetism Based on Intermediate Field Coupling Scheme

Jin-Ho Choy* and Jong-Young Kim

Department of Chemistry and Center for Molecular Catalysis, College of Natural Sciences, Seoul National University, Seoul 151-742, Korea
Received May 16, 1997

The magnetic susceptibilities of molybdenum ions with $4d^1$ electronic configuration in the octahedral crystal field were calculated on the basis of ligand field theory. The experimental magnetic susceptibilities for molybdenum ions, which are stabilized at the octahedral site in the perovskite lattice of $Ba_2ScMo^VO_6$ and $Sr_2YMo^VO_6$, were compared with the theoretical ones. We have tried to fit their temperature dependences of magnetic susceptibility with ligand field parameters, spin-orbit coupling constant ζ_{so}, and orbital reduction parameter κ according to intermediate field coupling and strong field theory. Strong field coupling theory could not explain experimental curves without unrealistically large axial ligand field, since it ignores the mixing up between different state via spin-orbit interaction and ligand field. On the other hand, the intermediate field coupling theory could successfully reproduce experimental data in octahedral and trigonal ligand field. The fitting result demonstrates not only the fact that spin-orbit interaction is primarily responsible for the variation of magnetic behavior but also the fact that effective orbital overlap, enhanced by cubic crystal structure, reduces significantly orbital angular momentum as indicated by κ parameter.

Introduction

In order to interpret the magnetic property of second and third row element, more rigorous calculation is required than the simplified one such as weak field coupling, which has been known to be quite successful in interpreting the magnetic property of first row element. There is a marked difference in the magnetic and optical properties between the $4d^n$ and $5d^n$ transition metal ions and $3d^n$ ones, since spin-orbit interaction as well as ligand field are much stronger than interelectronic repulsion in the former, compared to the latter.[1-7] In fact, in going from $3d$ toward $4d$ and $5d$, we notice that the interelectronic repulsion among the outer shell electrons gets weaker while the spin-orbit interaction becomes stronger. Therefore, the influences of spin-orbit interaction and ligand field need to be relevantly considered. As it is well-known, in the weak field coupling scheme, the starting orbital is d and the zeroth order wavefunctions are

$$|d, m_l=2>,\ |d, 1>,\ |d, 0>,\ |d, -1>,\ \text{and}\ |d, -2>$$

and the zeroth order Hamiltonian consists of the free ion Hamiltonian, given by

$$H_W = H_{core} - \sum_i \frac{Ze^2}{r_i} + \sum_{i \neq j} \frac{e^2}{r_{ij}}$$

where the summation is over all the d electrons. Here H_{core} involves the electrons in the closed shells. The symmetry group of H_W is the full rotation group R_3 in the weak field

*To whom all correspondence should be addressed

scheme. In the strong field scheme, the starting orbitals are t_2 and e. The zeroth order functions are

$$|t_2\xi> \ |t_2\eta> \ t_2\zeta> \ |e\theta> |e\varepsilon>$$

and the zeroth order Hamiltonian is given by

$$H_S = H_{core} - \sum_i \frac{Ze^2}{r_i} + \sum_i V_C + \sum_{i \neq j} \frac{e^2}{r_{ij}}$$

and the symmetry group of H_S is O_h. In the intermediate coupling scheme, the starting orbitals are γ_{8l}, γ_7, and γ_{8u}. The zeroth order Hamiltonian now includes the spin-orbit interaction:

$$H_I = H_{core} - \sum_i \frac{Ze^2}{r_i} + \sum_i V_C + \sum_{i \neq j} \frac{e^2}{r_{ij}} + \zeta \sum_i \boldsymbol{l}_i \cdot \boldsymbol{s}_i$$

Owing to the spin operators in the above Hamiltonian, the symmetry group of H_I is now the octahedral double group, denoted by O_h'.[7]

In this work, we have applied intermediate field coupling scheme and strong field one based on ligand field theory to the magnetic property of perovskite compounds, in which molybdenum ion possessing $4d^1$ electronic configuration is stabilized at the octahedral site. Comparison of the fitting results based upon intermediate field coupling and strong field one will give us how the nature of element such as spin-orbit coupling and bond covalency influences the magnetic behavior of the molybdenum in the lattice of perovskite oxide.

Experimental

The polycrystalline samples of Ba_2ScMoO_6 and Sr_2YMoO_6 have been prepared from high purity $BaCO_3$, $SrCO_3$, Sc_2O_3, Y_2O_3, and MoO_3 in flowing H_2 atmosphere. The stoichiometric mixtures were thoroughly ground in an agate mortar, and pelleted, and then heated. The single phase molybdenum compounds could be obtained by heat treatment at 1200 °C for 1hr. The oxidation state of molybdenum was determined by redox titration using cerium sulfate with ferroin indicator. Average oxidation numbers were obtained as 4.99 ± 0.04 and 5.00 ± 0.04 for Ba_2ScMoO_6 and Sr_2YMoO_6, respectively. The powder X-ray diffraction patterns for molybdenum compounds were collected at room temperature by step scanning with an increment of 0.02° (2θ) and a counting time of 6 sec, using Philips X'pert PW 1830 automated powder diffractometors with Ni filtered Cu-K_α radiation. Rietveld refinements were made with the program RIETAN-94. Experimental magnetic susceptibilities for both compounds were measured by means of an automatic DSM 8 type susceptometer in the temperature range from 10 K to 300 K. The equipment was calibrated using a single crystal of $Gd_2(SO_4)_3 \cdot 8H_2O$. Diamagnetic contribution of every ion was corrected according to Selwood.[8] UV-Visible-NIR spectra were recorded in the diffuse reflectance mode at room temperature on Perkin-Elmer lamda 12 spectrophotometer with integrating sphere. Although the crystal structure of Sr_2YMoO_6 was reported to have pseudo cubic crystal system,[9] we have found that it has monoclinic structure with the space group of $P2_1/n$. Most of the strong peaks in the diffraction pattern for Sr_2YMoO_6 seem to be indexed by an ordered perovskite structure in the cubic space group $Fm\bar{3}m$ with a doubled unit cell parameter of a simple perovskite lattice, but some peaks with very low intensity could not be indexed with this space group. And, as shown in Figure 2-(c), body-centered orthorhomic structure (*Pnnm*) could not successfully index all of peaks and the splitting of peaks in high angle range could not successfully reproduced. Careful analysis of all the diffraction lines indicates that the crystal symmetry is reduced to a monoclinic $P2_1/n$ space group. This space group permit ordering of Y and Mo cations over 6-coordinate sites of perovskite structure. And it should be noted that the lattice parameters can be considered as those of a body-centered orthorhombic lattice, and the B-site cations retain the body-centered orthorhombicity, but only the Sr and oxygen ions lose the orthorhombic symmetry, so that the lattice symmetry was reduced to a monoclinic one. Although the crystal system of Ba_2ScMoO_6 was described as hexagonal one in the previous report,[10] there is no evidence on the lowering of symmetry from cubic symmetry in the present X-ray diffraction pattern. According to the refinement, R_{wp} values are lowered to 6.95% and 5.02% for Ba_2ScMoO_6 and Sr_2YMoO_6, respectively. Finally refined parameters and selected bond distances and angles are presented in Tables 1 and 2, respectively. Crystal structures

Table 1. Crystallographic data for cubic Ba_2ScMoO_6 and monoclinic Sr_2YMoO_6 with standard deviation in parentheses

Atom	Site	x	y	z	Occupancy	B (Å^2)
			Ba_2ScMoO_6			
Ba	1a	0	0	0	1	0.67 (20)
Sc	1b	1/2	1/2	1/2	1	0.67 (20)
Mo	1b	1/2	1/2	1/2	1	0.67 (20)
O	3c	1/2	1/2	0	1	0.67 (20)
			Sr_2YMoO_6			
Sr	4e	0.000 (2)	0.029 (0)	0.745 (1)	1	0.68 (4)
Y	2d	1/2	0	0	1	0.68 (4)
Mo	2c	0	1/2	0	1	0.68 (4)
O1	4e	0.274 (7)	0.307 (7)	-0.025 (5)	1	0.68 (4)
O2	4e	0.298 (7)	0.256 (6)	0.525 (6)	1	0.68 (4)
O3	4e	-0.094 (5)	0.492 (3)	0.765 (5)	1	0.68 (4)

	Ba_2ScMoO_6	Sr_2YMoO_6
cell parameter	a=4.0841 (1) Å	a=5.7985 (2) Å, b=5.8242 (1) Å c=8.2095 (2) Å, β=90.217° (2)
Space group	$Pm\bar{3}m$ (no. 221)	$P2_1/n$ (no. 14)
Number of parameters	21	35
2θ range	10°-120°	15°-100°
R-factors[1)]	R_p=5.42% R_{exp}=3.79% R_{wp}=6.95% S=1.8325	R_p=3.60% R_{exp}=3.00% R_{wp}=5.02% S=1.6744

$R_p = 100 \times \Sigma|Y_{obs}-Y_{calc}|^2/\Sigma Y_{obs}$
$R_{wp} = 100 \times \Sigma w|Y_{obs}-Y_{calc}|^2/\Sigma w|Y_{obs}|^2$
$R_{exp} = 100 \times (N-P+C)/\Sigma w|Y_{obs}|^2$
$S = R_{wp}/R_e$
Y_{obs}=observed intensity, Y_{cal}=calculated intensity and N-P+C= number of observations-number of variables+number of constraints.

Table 2. Selected interatomic distances (Å) and bond angles (°) for molybdenum perovskites

Compounds	Mo-O distance (Å) B-O distance (Å)	O-Mo-O bond angle (°) Mo-O-B bond angle (°)
Ba_2ScMoO_6	Mo-O 2.042 (1)	O-Mo-O 180
	Sc-O 2.042 (1)	Mo-O-Sc 180
Sr_2YMoO_6	Mo-O1 1.96 (4)×2	O1-Mo-O2 93 (2)
	Mo-O2 1.93 (4)×2	O1-Mo-O3 84 (1)
	Mo-O3 2.00 (4)×2	O2-Mo-O3 94 (2)
	Y-O1 2.23 (4)×2	Y-O1-Mo 159 (2)
	Y-O2 2.22 (3)×2	Y-O2-Mo 163 (2)
	Y-O3 2.25 (4)×2	Y-O3-Mo 150 (2)

of cubic Ba_2ScMoO_6 and monoclinic Sr_2YMoO_6 are shown in Figure 1. The observed, calculated, and difference profiles are shown in Figure 2.

Ligand Field Calculation

In the strong field coupling scheme, in which the spin-orbit interaction is not included in zeroth order Hamiltonian, there are two single-electron levels denoted by t_2 (lower level) and e (upper level) whose spatial degeneracies are 3 and 2, respectively. The sets of spatial basis functions for these two levels are (ξ, η, ζ) and (θ, ε) with a spin degeneracy of

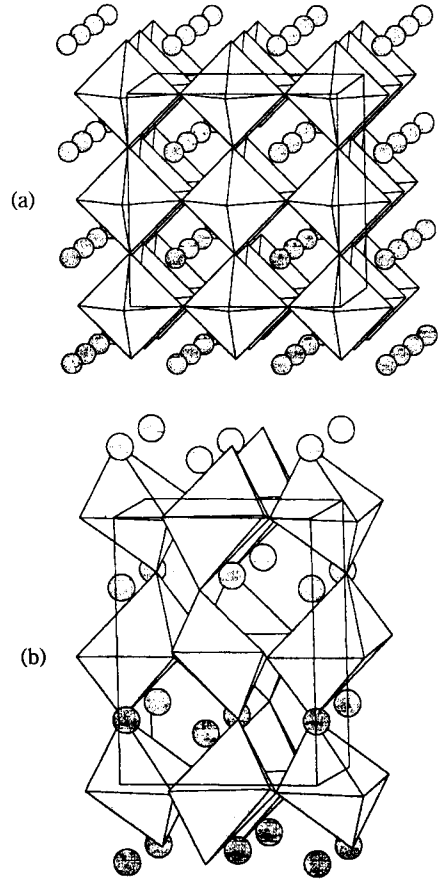

Figure 1. (a) Cubic crystal structure of Ba_2ScMoO_6. Filled circles and octahedra represent barium, ScO_6, and MoO_6, respectively. (b) Monoclinic crystal structure of Sr_2YMoO_6.

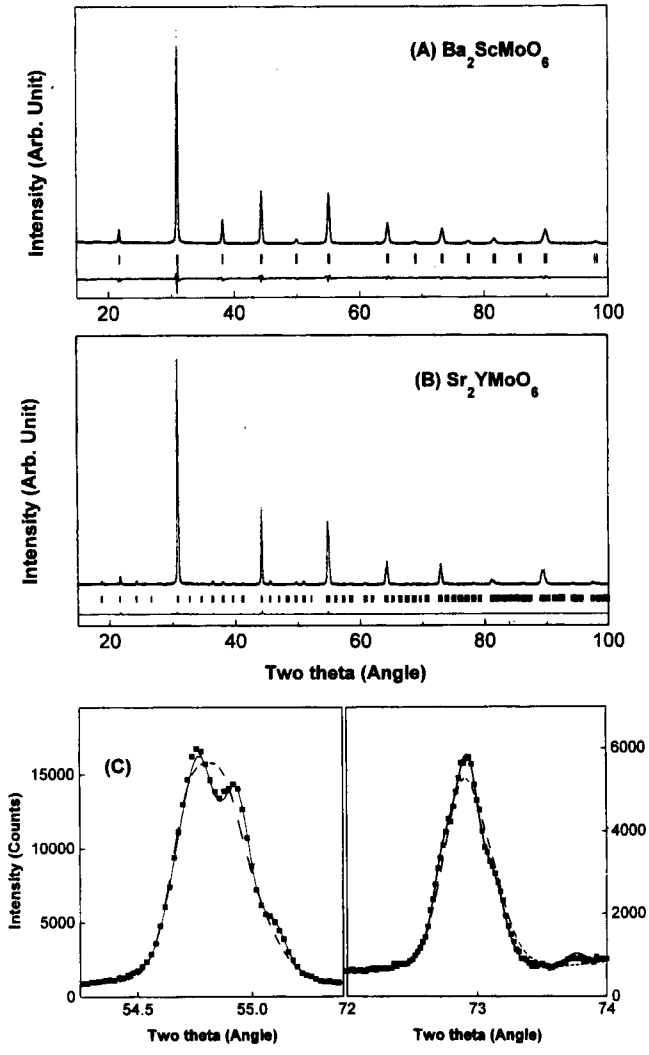

Figure 2. X-ray powder diffraction patterns for (a) Ba_2ScMoO_6 and (b) Sr_2YMoO_6. Observed (+), calculated (−), difference (−) profiles and Bragg positions (|) for Ba_2ScMoO_6 and Sr_2YMoO_6 are presented. (c) The observed (■) and calculated profiles based on the orthorhombic (*Pnnm*; dashed line) and monoclinic ($P2_1/n$; solid line) space group are compared.

2, respectively, which span the T_{2g} and E_g representations of the O_h group.[7] These functions are suitable linear combinations of the five d orbitals (d_2, d_1, d_0, d_{-1}, d_{-2}). The electronic energies for the t_2 and e levels are, respectively, $-4Dq$ and $6Dq$ measured from the free ion energy level. The effects of tetragonal crystal field and spin-orbit coupling were treated as simultaneous perturbations, which are represented in Table 5 by Δ and ζ_{so} as an indication of respective interaction. Spin-orbit interaction parameter ζ_{so} should not be confused with the spatial basis function ζ. The effect of a magnetic field, which causes changes in energy which are considerably smaller than the previous perturbations, is then treated as a further perturbation.[11]

The complete sets of basis functions in the intermediate field coupling are obtained by coupling of spatial basis functions, (ξ, ζ, η) and (θ, ε) for t_2 and e, respectively, with the spin functions. And then the symmetry adapted irreducible representations Γ_7 and Γ_8 of the double group O_h' could be

Table 3. Symmetry adapted wavefunctions for d^1 configuration

Terms	Wavefunctions
$\Gamma_8'(^2T_{2g})$	$\Gamma_8\,\frac{3}{2}> = \frac{i}{\sqrt{6}}\,\xi^+ + \frac{1}{\sqrt{6}}\,\eta^+ + \frac{i\sqrt{2}}{\sqrt{3}}\,\zeta^-$
	$\Gamma_8\,\frac{1}{2}> = \frac{-i}{\sqrt{2}}\,\xi^- - \frac{1}{\sqrt{2}}\,\eta^-$
	$\Gamma_8\,\frac{-1}{2}> = \frac{i}{\sqrt{2}}\,\xi^+ - \frac{1}{\sqrt{2}}\,\eta^+$
	$\Gamma_8\,\frac{-3}{2}> = \frac{-i}{\sqrt{6}}\,\xi^- + \frac{1}{\sqrt{6}}\,\eta^- + \frac{i\sqrt{2}}{\sqrt{3}}\,\zeta^+$
$\Gamma_7(^2T_{2g})$	$\Gamma_7\,\frac{-1}{2}> = \frac{-1}{\sqrt{3}}\,\xi^+ - \frac{1}{\sqrt{3}}\,\eta^+ + \frac{i}{\sqrt{3}}\,\zeta^-$
	$\Gamma_7\,\frac{1}{2}> = \frac{-1}{\sqrt{3}}\,\xi^- + \frac{1}{\sqrt{3}}\,\eta^- - \frac{i}{\sqrt{3}}\,\zeta^+$
$\Gamma_8''(^2E_g)$	$\Gamma_8'\,\frac{3}{2}> = \varepsilon^-$
	$\Gamma_8'\,\frac{1}{2}> = -\theta^+$
	$\Gamma_8'\,\frac{-1}{2}> = \theta^-$
	$\Gamma_8'\,\frac{-3}{2}> = -\varepsilon^+$

where,

$\xi = \frac{i}{\sqrt{2}}\,(|1>+|-1>) = d_{yz}$

$\eta = \frac{-1}{\sqrt{2}}\,(|1>-|-1>) = d_{xz}$

$\zeta = \frac{-i}{\sqrt{2}}\,(|2>+|-2>) = d_{xy}$

$\theta = |0> = d_{z^2}$

$\varepsilon = \frac{1}{\sqrt{2}}\,(|2>+|-2>) = d_{x^2-y^2}$

obtained. Since the spin functions

$$|S=\frac{1}{2},\ m_S=+\frac{1}{2}> \text{ and } |S=\frac{1}{2},\ m_S=-\frac{1}{2}>$$

span the Γ_6 representation of O_h', Γ_8 and Γ_7 can be obtained after decomposition of the direct product $T_{2g} \otimes \Gamma_6$, which give the two sets in Table 3. Similarly $E_g \otimes \Gamma_6$ gives the next set. The coupling coefficients required here are given in Table A20 of reference 12.

In the presence of the spin-orbit interaction term $\boldsymbol{l}\cdot\boldsymbol{s}$, there will be a mixing between the Γ_{8t_2} and Γ_{8e} terms. The matrix of H_0 between these two terms is as follows:

$$H_0 = \begin{array}{c} \\ \Gamma_{8t_2} \\ \Gamma_{8e} \end{array} \begin{array}{c} \begin{array}{cc} \Gamma_{8t_2} & \Gamma_{8e} \end{array} \\ \begin{pmatrix} -4Dq - \frac{1}{2}\,\zeta_{so} & \sqrt{3/2}\,\zeta_{so} \\ \sqrt{3/2}\,\zeta_{so} & 6Dq \end{pmatrix} \end{array}$$

Diagonalization of the above matrix gives two eigenvalues,

$$\varepsilon_0(8l) = Dq - 1/4\,\zeta_{so} - 1/62\,[910Dq + 1/2\zeta_{so})^2 + 6\zeta_{so}^2]^{1/2}$$
$$\varepsilon_0(8u) = Dq - 1/4\,\zeta_{so} - 1/62\,[910Dq + 1/2\zeta_{so})^2 + 6\zeta_{so}^2]^{1/2}$$

with the corresponding eigenvectors

$$\begin{pmatrix} \cos\theta \\ -\sin\theta \end{pmatrix} \quad \begin{pmatrix} \sin\theta \\ \cos\theta \end{pmatrix}$$

Table 4. Energy matrix for Γ_4, Γ_5 and Γ_6 states in D_{3d}'

Γ_4	$\Gamma_7(^2T_{2g})$	$\Gamma_8(^2T_{2g})$	$\Gamma_7(^2E_g)$
	$\zeta_{so} - 4Dq - \frac{14}{9}\,D\tau$	$\frac{\sqrt{2}}{9}\,(9D\sigma + 20D\tau)$	$\frac{2}{3\sqrt{3}}\,(2D\sigma - 5D\tau)$
		$-\frac{1}{2}\,\zeta_{so} - 4Dq - \frac{1}{9}$	$\sqrt{\frac{3}{2}}\,\zeta_{so} + \frac{\sqrt{2}}{3\sqrt{3}}$
		$(9D\sigma + 34D\tau)$	$(2D\sigma - 2D\tau)$
			$6Dq + \frac{7}{3}\,D\tau$

Γ_5, Γ_6	$\Gamma_8(^2T_{2g})$	$\Gamma_8(^2E_g)$
	$-\frac{1}{2}\,\zeta_{so} - 4Dq + D\sigma + \frac{3}{2}\,D\tau$	$\sqrt{\frac{3}{2}}\,\zeta_{so} - \frac{\sqrt{2}}{3}\,e^{i\beta/2}$
		$(2D\sigma - 5D\tau)$
		$6Dq + \frac{7}{3}\,D\tau$

where,

$\cos\beta = -\frac{1}{3},\ \sin\beta = \frac{2\sqrt{2}}{3}$

respectively, where

$$\tan\theta = \frac{\sqrt{6}\,\zeta_{so}}{10Dq + \frac{1}{2}\,\zeta_{so}}$$

Now, the Γ_{8l} and Γ_{8u} basis sets corresponding to the two fourfold degenerate energy levels in energy matrix are linear combinations of the original Γ_{8t_2} and Γ_{8e} basis sets;

$$a_l = |\Gamma_{8l}a> = 6\cos\theta\,|\,\Gamma_{8t_2}a> - \sin\theta\,|\,\Gamma_{8e}a>$$
$$a_u = |\Gamma_{8u}a> = 6\sin\theta\,|\,\Gamma_{8t_2}a> + \cos\theta\,|\,\Gamma_{8e}a>$$

The Γ_{8u} level is above the Γ_{8l} level and the remaining doubly degenerate Γ_7 level lies in between those two. The energy value of the Γ_7 level is

$$\varepsilon_0(\Gamma_7) = <\Gamma_7 a\,|\,H_O\,|\,\Gamma_7 a> = -4Dq + \zeta_{so}$$

The levels in O_h ligand field are further split by trigonal ligand field interaction, and five Kramer's doublet belonging to the irreducible representation Γ_4, Γ_5, and Γ_6 of the trigonal double group D_{3d}' can be obtained.[2,7] The irreducible representation Γ_4 is doubly degenerate, whereas Γ_5 and Γ_6 are nondegenerate. But, these nondegenerate representations are Kramer's conjugate and constitute a Kramer's doublet. The energy matrices for Γ_4, Γ_5, and Γ_6 states have been reported in Table 4. After the energy matrices were diagonalized to obtain the energy and the zeroth order wavefunctions, three doubly degenerated terms at the lower energy level were used. From these three doubly degenerate wavefunctions, the matrices of parallel and perpendicular magnetic moments and 1st and 2nd order Zeeman coefficients could be derived with the orbital ($\boldsymbol{l}_i$) and spin ($\boldsymbol{s}_i$) operators.[13] Orbital reduction factors κ and κ' were defined as a measure of quenching of orbital angular momentum within t_{2g} orbitals and between t_{2g} and e_g orbitals, respectively. Finally, the magnetic susceptibility χ_i (i=x, y, z) could be calculated using Van Vleck's equation.[1] Electronic states of Mo^V ion ($4d^1$) in octahedral symmetry are described in Figure 3. The UV-Visible-NIR diffuse reflectance spectra of Mo^V compounds in the range of 300 nm-700 nm

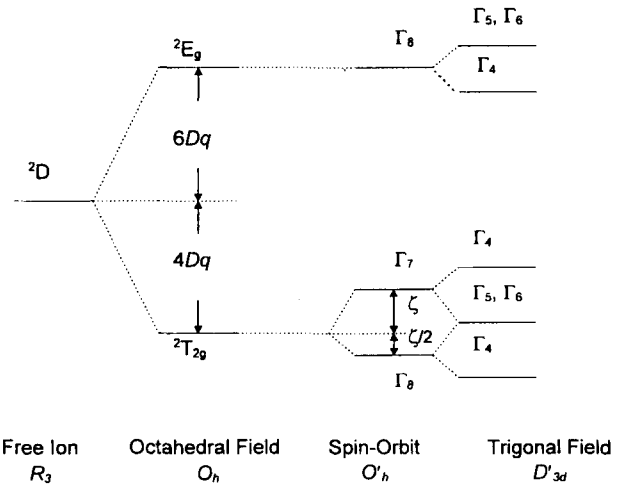

Figure 3. Schematic electronic states of Mo^V ion ($4d^1$) in octahedral symmetry.

are shown in Figure 4. Ligand field parameter Dq was constrained to be 2850 cm^{-1} according to the bands around 350 nm, and the other parameters were obtimized as variables in the nonlinear least-squares fitting procedure. The result of best-fit between the experimental magnetic susceptibilities and the calculated ones is shown in Figure 5, and the fitted parameters are summarized in Table 5.

Discussion

For the molybdenum belonging to second transition metal series, it is necessary to consider the mixing between t_2 and e level *via* spin-orbit interaction and crystal field. In this point of view, it is expected that the intermediate field coupling theory, in which spin-orbit interaction matrices could be completely diagonalized, could give us more physically meaningful parameters. For Ba_2ScMoO_6 with cubic crystal

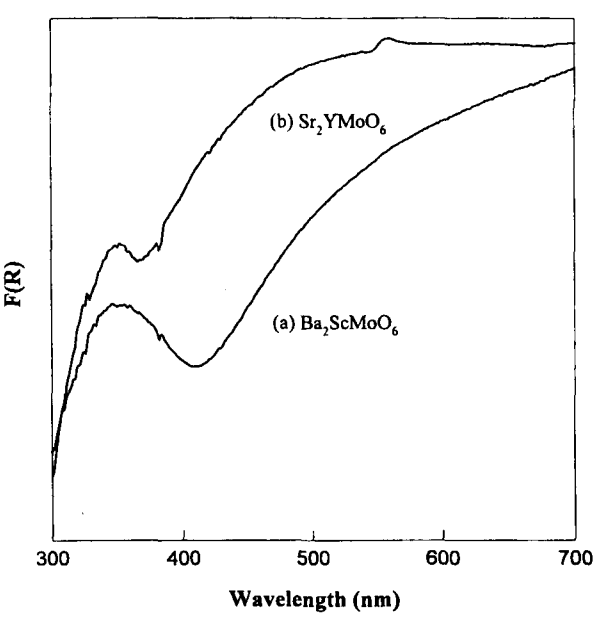

Figure 4. Diffuse reflectance spectra for (a) Ba_2ScMoO_6 and (b) Sr_2YMoO_6.

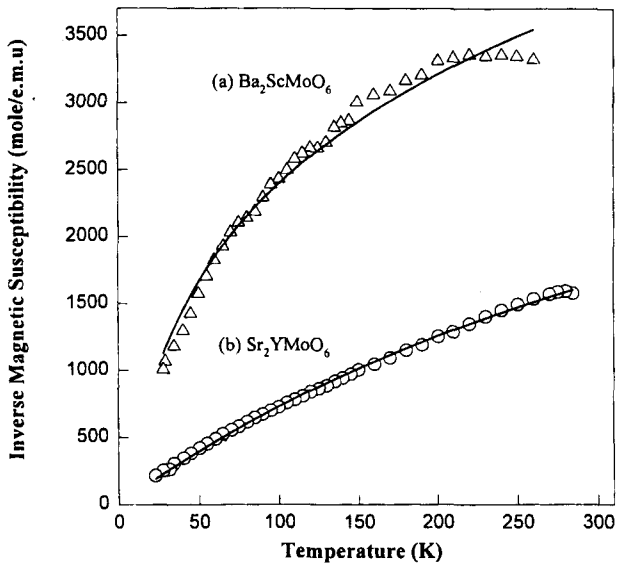

Figure 5. (a) Experimental (△) and theoretical (−) magnetic susceptibilities for Ba_2ScMoO_6. (b) Experimental (○) and theoretical (−) ones for Sr_2YMoO_6.

structure, the theoretical calculation of magnetic susceptibility based on the strong field coupling could not give satisfactory fitting with experimental data without axial field parameter Δ (550 cm^{-1}), whereas that based on the intermediate field coupling is in good agreement with the experimental one. It is therefore concluded that the latter theory is more appropriate than the former one in the case of molybdenum. For Sr_2YMoO_6 with monoclinic crystal structure, the ligand field of cubic symmetry does not explain experimental curve without extreme reduction of orbital angular momentum (κ=~0.2). Although we have tried to fit the experimental data by assuming a tetragonal distortion from cubic symmetry (*Ds*, *Dt*=0 or *Dσ*, *Dτ*=0), the calculation under the action of tetragonal ligand field does not give any satisfactory agreement with the observed magnetic susceptibility without unrealistically large tetragonal field parameters *Ds* and *Dt*, as much as 400-800 cm^{-1}, and extreme reduction of κ parameter (κ=0.1-0.3). On the other hand, the calculation assuming the action of trigonal field gives reasonable fitting result. Trigonal field parameters *Dσ* and *Dτ* were assumed to be equal, and *Dq* parameter for each compound was constrained according to the bands around 350 nm in optical spectra as shown in Figure 4, which are due to vibronically allowed *d-d* transitions ($t_{2g} \rightarrow e_g^a$). As the band corresponding to *d-d* transition does not exhibit discernible variation, the ligand field parameters *Dq* for both molybdenum compounds were set equal to 2850 cm^{-1}.

According to the magnetic susceptibility fitting result, the

Table 5. Summary of magnetic susceptibility best-fit results

Compounds	Intermediate coupling				Strong field		
	Dσ, *Dτ* (cm^{-1})	ζ_{so} (cm^{-1})	κ	κ'	Δ (cm^{-1})	ζ_{so} (cm^{-1})	κ
Ba_2ScMoO_6	*Dσ*=*Dτ*=0	950	0.86	0.55	550	996	1.00
Sr_2YMoO_6	*Dσ*=*Dτ*=131	704	1.0	0.75	897	649	1.00

spin-orbit coupling constant for Sr_2YMoO_6 (ζ_{so}=704 cm^{-1}) is more reduced than that for Ba_2ScMoO_6 (ζ_{so}=950 cm^{-1}), which implies that the (Mo-O) bond for Sr_2YMoO_6 is more covalent than that for Ba_2ScMoO_6.[7,11-13] The spin-orbit coupling constant for free Mo^V ion is known to be 1030 cm^{-1}.[14] This result could be explained by considering the local structure of the molybdenum site. It is expected that more acidic scandium will reduce (Mo-O) bond covalency because (B-O) bond (B=Sc, Y) competes with (Mo-O) bond by the pathway of 180°.[15] According to Rietveld refinement, the bond distance between molybdenum and oxygen for Ba_2ScMoO_6 (2.042 (1) Å) is larger than the average value of 1.96 Å for Sr_2YMoO_6 (1.93 (4), 1.96 (4), and 2.00 (4) Å), as shown in Table 2, which supports the magnetic susceptibility fitting result. The trend of orbital reduction factor could be explained by crystal structure. Smaller reduction of κ parameter in Sr_2YMoO_6 (κ=1.00, κ'=0.75) than Ba_2ScMoO_6 (κ=0.86, κ'=0.55) implies the fact that distorted crystal structure disturbs effective orbital overlap between molybdenum and oxygen.

Acknowledgment. This work was in part supported by the Korean Ministry of Science and Technology through the international collaboration program and by KOSEF through the center for molecular catalysis.

References

1. Van Vleck, J. H. *The Theory of Electric and Magnetic Susceptibilities*; Oxford University Press: London, 1965.
2. Liehr, A. D. *J. Phys. Chem.* **1960**, *64*, 43.
3. (a) De, I.; Desai, V. P.; Chakravarty, A. S. *Phys. Rev. B* **1973**, *8*, 3769. (b) Basu, S.; Chakravarty, A. S. *Phys. Rev. B.* **1982**, *26*, 4327. (c) Basu, S.; Chakravarty, A. S. *Phys. Rev. B.* **1983**, *27*, 6495.
4. Rahman, H. U. *Phys. Rev. B.* **1971**, *3*, 729.
5. Johannesen, R. B.; Candela, G. A. *Inorg. Chem.* **1963**, *2*, 67.
6. Kamimura, H.; Koide, S.; Sekiyama, H.; Sugano, S. *J. Phys. Soc. Jpn.* **1960**, *15*, 1264.
7. Chakravarty, A. S. *Introduction to the Magnetic Properties of Solids*; 1st ed.; John Wiley & Sons: New York, 1980.
8. Selwood, P. W. *Magnetochemistry*; 2nd ed.; Interscience: New York, 1956.
9. Kamata, K.; Yoshimura, M.; Nakamura, T.; Sata, T. *Chem. Lett.* **1972**, 1201.
10. Brandle, C. D.; Steinfink, H. *Inorg. Chem.* **1971**, *10*, 922.
11. Mabbs, F. E.; Machin, D. J. *Magnetism and Transition Metal Complexes*, 1st ed.; Halsted Press: New York, 1973; Chap 5.
12. Griffith, J. S. *The Theory of Transition Metal Ions*; Cambridge University Press : London, 1980.
13. Sugano, S.; Tanabe, Y.; Kamimura, H. *Multiplets of Transition Metal Ions in Crystals*; Academic press: New York, 1970.
14. Dunn, T. M. *Trans. Faraday. Soc.* **1961**, *57*, 1441.
15. (a) Choy, J. H.; Demazeau, G.; Byeon, S. H.; Dance, J. M. *J. Phys. Chem. Solids.* **1990**, *51*, 391. (b) Choy, J. H.; Demazeau, G.; Dance, J. M. *J. Solid. State. Chem.* **1990**, *84*, 1. (c) Choy, J. H.; Park, J. H.; Hong, S. T.; Kim, D. K. *J. Solid. State. Chem.* **1994**, *111*, 370.

Ab initio Nuclear Shielding Calculations for Some X-Substituted Silatranes Using Gauge-Including Atomic Orbitals

Dong Hee Kim* and Mi Jung Lee

Department of Chemistry, Kunsan National University, Kunsan 573-701, Korea
Received May 17, 1997

^{13}C, ^{15}N, and ^{29}Si NMR chemical shifts have been computed for selected X-substituted silatranes (X=Cl, F, H, CH_3) using Gauge-Including Atomic Orbitals (GIAO) at the Hartree-Fock level of theory. The isotropic ^{13}C chemical shifts are largely insensitive to substituent-induced structural changes. In this study, the isotropic ^{13}C chemical shifts between 1-methyl- and 1-hydrogensilatranes by GIAO-SCF calculation at the HF/6-31G level are very similar. But the results of 1-chloro- and 1-fluorosilatranes are about 4 ppm different from the experimental values. In contrast, the isotropic ^{15}N and ^{29}Si chemical shifts and the chemical shielding tensors are quite sensitive to substituent-induced structural changes. These trends are consistent with those of the experiment. The isotropic ^{15}N chemical shift demonstrates a very clear correlation with Si-N distance. But in case of ^{29}Si the correlations are not as clean as for the ^{15}N chemical shift; the calculated variation in the ^{29}Si chemical shift is much larger.

Introduction

The isotropic chemical shift is an immensely useful parameter in the determination of chemical structure. This usefulness is largely due to empirical structure/chemical shift correlations. However, the problem of the understanding of the relationship between the chemical shift and molecular structure can be quite difficult. *Ab initio* calculations are

*Author to whom correspondence should be addressed.